

Nuclear pores in luteal cells during pregnancy and after parturition and pup removal in the rat. A freeze-fracture study

JUAN CARLOS CAVICCHIA*, GUSTAVO GUEMBE, MABEL FÓSCOLO

Instituto de Histología y Embriología "Dr. Mario H. Burgos" (IHEM). CONICET. Facultad de Ciencias Médicas. Universidad Nacional de Cuyo. Argentina.

Key words: apoptosis, corpus luteum, nuclear envelope, nucleocytoplasmic transport

ABSTRACT: In a previous paper we described a pronounced increase of apoptotic nuclei in rat corpus luteum of pregnancy whose programmed chromatin degeneration was induced by the progesterone antagonist mifepristone. Those observations encouraged us to study the apoptotic nuclear membrane during pregnancy and after parturition and pup removal, by using a freeze-fracture technique which allows us to observe 'en face' the nuclear envelope and also permits nuclear pore counting. This study was complemented with the TUNEL assay (TdT-mediated dUTP nick-end labelling). Changes in nuclear pores during pregnancy begin with an intense reduction in number but still showing an even distribution on the nuclear membrane, never forming aggregations sharply separated from pore-free areas, which are characteristic of other apoptotic models. Electron microscopy of thin-sections shows, coincidentally with findings in the freeze-fracture replicas, a moderately irregular aggregation of marginal heterochromatin condensations. After nuclear fragmentation and micronuclear formation, pores behave in the usual manner in other apoptotic models, i.e., mainly showing migrations of nuclear pores toward the chromatin-free areas. The present results support the hypothesis that nuclear pore complexes are dynamic structures, which permit their migration toward nuclear membrane areas devoid of chromatin aggregations that might block the nucleocytoplasmic transport in such areas.

Introduction

Since the early study of Friend and Fawcett (1974) using thin sectioning correlated with freeze-fracture techniques, it has been recognized that freeze-fracture is a valuable method to study cell membranes 'en face' with their associated particles, such as membrane receptors, channels and pores. It also permits a morphometric analysis of nuclear pore dimension, shape, number, distribution and density.

In a previous freeze fracture study of seminiferous tubules we have observed a characteristic pore aggrega-

tion in germ cells from spermatogonia to spermatids (Cavicchia and Morales, 1992). This behavior appeared related to the degree of nucleocytoplasm transport at each germ cell stage. In another report, we have also shown that Sertoli cells vary both in the degree of nuclear pore aggregation and in pore density, according to the degree of nucleocytoplasm transport, also dependent of the metabolic activity of each Sertoli cell in a given stage of differentiation of the seminiferous epithelium (Cavicchia *et al.*, 1998). The correlation between pore number and metabolic activity was previously reported by others in several biological models (Aldrich and Pendland, 1981; Maul *et al.*, 1972).

Falcieri *et al.* (1994) have studied nuclear pore behavior in five different apoptotic models showing a constant migration of nuclear pores towards the diffuse

*Address correspondence to: Juan Carlos Cavicchia.

E-mail: jccavic@fcm.uncu.edu.ar

Received: October 7, 2009. Revised version received: February 23, 2010. Accepted: July 8, 2010.

chromatin areas and the formation of a vast heterochromatin area devoid of nuclear pores, exhibiting a compact chromatin margination towards a nuclear pole where it appears cap-shaped, uniformly electron-dense and sharply separated from the rarefied chromatin areas (Falcieri *et al.*, 1994). As a consequence, intense pore clumping was observed in these models.

In a previous paper (Telleria *et al.*, 2001), we reported the apoptotic chromatin behavior of luteal cells induced by the progesterone antagonist mifepristone (RU 486), and found evenly distributed heterochromatin condensations under the nuclear envelope, which is in contrast with other known apoptotic models. Also, this peculiar apoptotic behavior encouraged us to study the corpus luteum of postpartum rats in which the pups were removed, since according to Takiguchi *et al.* (2004), prolactin withdrawal caused by pup removal also induces dramatic apoptotic changes in this ephemeral gland.

Material and Methods

Animals and groups

Wistar rats used in the present work were kept in the animal room on a 12-hr light/12-hr dark regime and were fed *ad libitum* on a commercial rodent chow and water. The Guidelines for the Care and Use of Laboratory Animal (National Institutes of Health, Bethesda MD) were followed.

Female rats were caged individually with fertile males in the afternoon of proestrus, and positive matings were verified by sperm in the vagina on the following

morning. That day was designated day 0 of pregnancy. Rats of our colony give birth usually on day 22, and the pups were removed on this day.

Three experimental groups (5 rats each) were used, *i.e.*, (1) day 15 of pregnancy, (2) day 21 of pregnancy; and (3) day 5 after parturition and pup removal. Animals were sacrificed under ether anesthesia, and one of the largest corpora lutea was immediately removed from each rat and processed for either light or electron microscopy.

Detection of apoptosis

An apoptosis specific assay (the terminal deoxynucleotidyl transferase-mediated dUTP nick end labelling, TUNEL) was used as previously described (Sinha Hikim *et al.*, 1997; Morales *et al.*, 2007). Corpora lutea were fixed in 5% glutaraldehyde (TAAB; U.K.) in phosphate buffer-saline, dehydrated in a progressive ethanol series, embedded in paraffin and 5-10 μm sections were obtained, and processed with the Dead End colorimetric TUNEL system (Promega) to detect DNA strand breaks with the peroxidase and diaminobenzidine colorimetric reaction (Gavrieli *et al.*, 1992). As a negative control, tissue sections were processed in an identical manner, except that terminal deoxynucleotidyl transferase (TdT) enzyme was replaced by the same volume of distilled water.

Electron microscopy

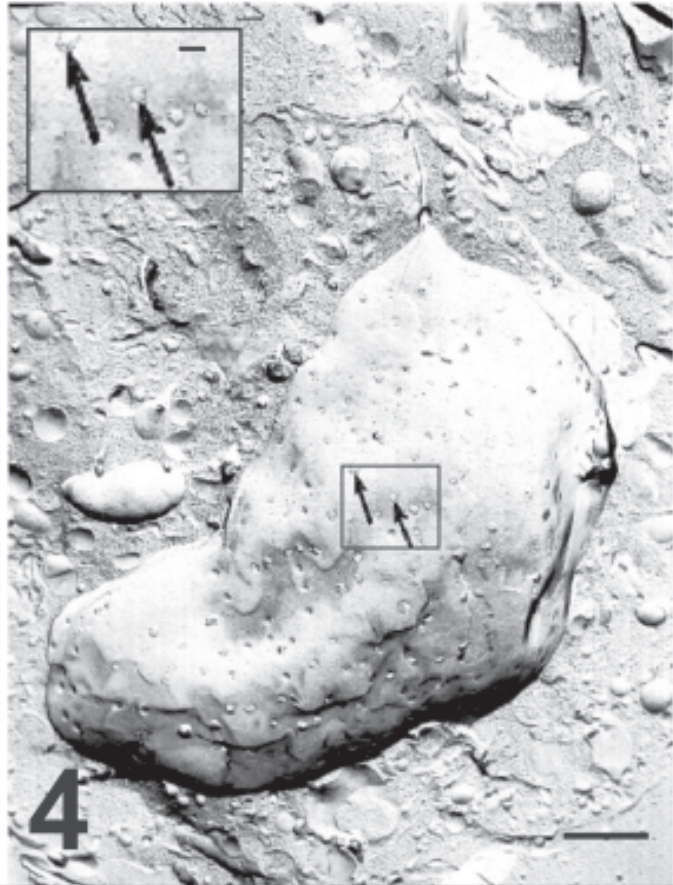
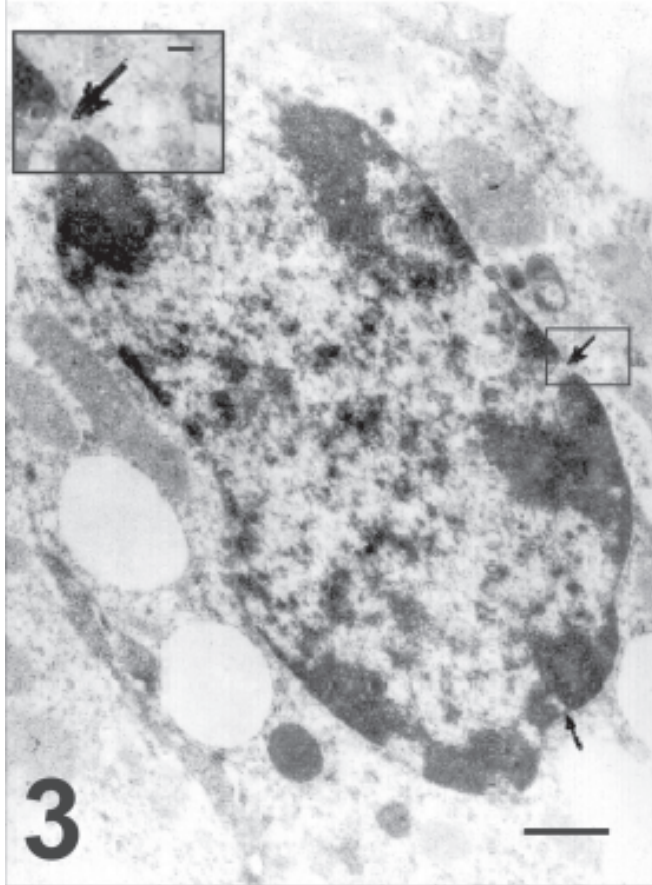
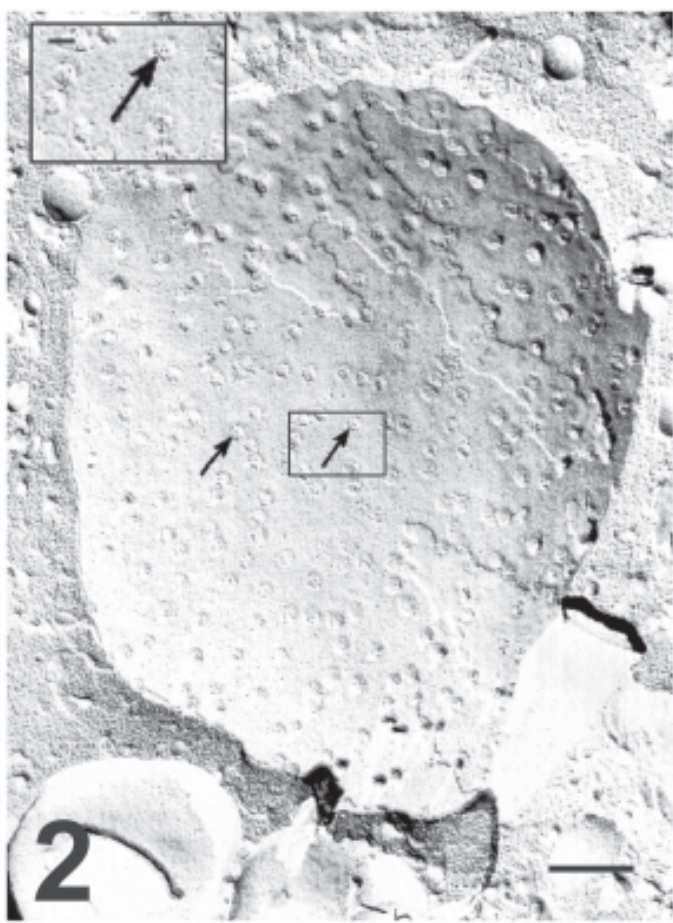
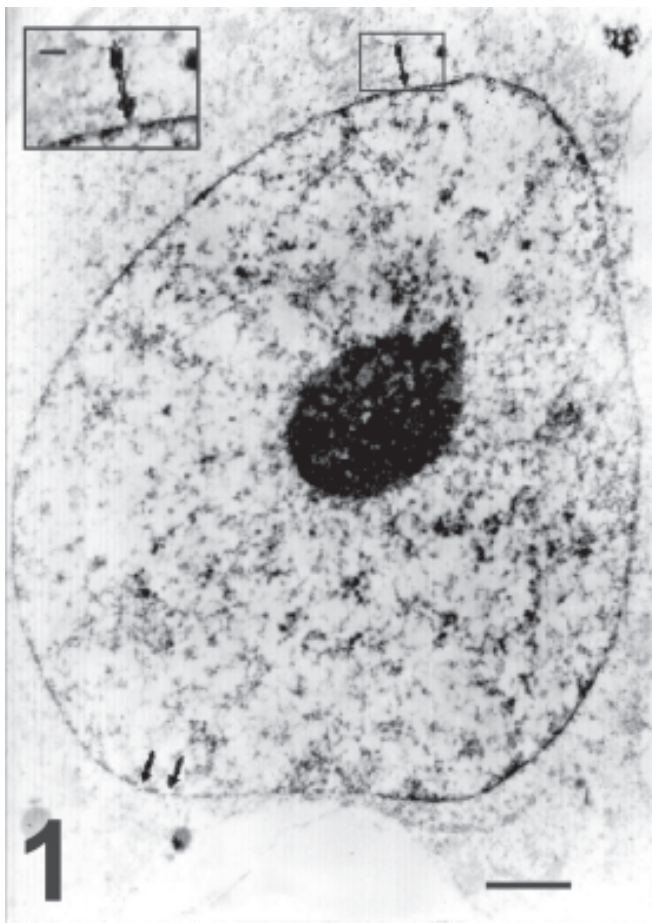
Small corpus luteum pieces were cut using a razor blade, placed in 5% glutaraldehyde buffered with 0.1

FIGURE 1. Ultrastructure of an endocrine luteal cell without signs of apoptosis on day 15 of pregnancy. Chromatin is evenly distributed. Arrows indicate nuclear pores homogeneously distributed on the nuclear membrane. Bar represents 2 μm . The inset shows a nuclear pore at higher magnification. Bar represents 0.75 μm .

FIGURE 2. Freeze-fracture of a cell similar to that shown in the preceding figure. Arrows point to numerous nuclear pores, evenly distributed on the nuclear membrane. Bar represents 2 μm . Notice that with the freeze fracture preparation nuclear diameter size is similar to electron microscopy and thin section preparation. The inset shows a membrane area at higher magnification and its bar represents 0.75 μm .

FIGURE 3. Electron micrograph of a luteal cell likely at the beginning of apoptotic degeneration on day 15 of pregnancy. The nucleus is highly deformed. There are numerous small and condensed chromatin clumps, which are evenly distributed in the nucleoplasm, while some large chromatin patches appear attached to the nuclear envelope. Arrows indicate nuclear pores, which appear located between the condensed chromatin patches. Notice that nuclear diameter is about 15-20 μm . Bar represents 2 μm . The inset shows at higher magnification one of these pores (arrow), opened between two apoptotic chromatin clusters. Bar represents 0.75 μm .

FIGURE 4. Freeze fracture of a luteal cell similar to the one shown in the previous figure. A decreased density of nuclear pores (arrows) in an even distribution is evident, as compared to the control cell (Fig. 2). Bar represents 2 μm . The inset shows nuclear pores at higher magnification (arrows). Bar represents 0.75 μm .



M sodium cacodylate, pH 7.4 for 4 hr, postfixed in 1% osmium tetroxide in the same buffer with 1% potassium ferrocyanide as an auxiliary membrane contrast substance (Karnovsky, 1971), dehydrated in graded series of acetone and embedded in low viscosity resin (Pelco International, CA) as described by Spurr (1969). One μm sections were stained with toluidine blue-sodium borate for topographical orientation. Ultrathin sections were stained with uranyl acetate and lead citrate (Reynolds, 1963) and examined in a Zeiss 902 electron microscope.

Freeze-fracture study

Small corpus luteum pieces were fixed in glutaraldehyde-cacodylate buffer at room temperature (18°C) for 2 h, and then immersed in 30% glycerol for 2 h. Afterwards they were mounted on gold supports and quickly frozen in Freon 22 and liquid nitrogen. Freeze-fracture replicas of platinum-carbon were obtained in a Balzers BAF 301 apparatus at -100°C. Replica thickness was checked with a quartz film monitor. Cleaning and degreasing was performed with commercial bleach. Replicas were supported on nickel grids. Observations were carried out in a Zeiss 902 electron microscope.

For random sampling, all regions of each replica containing nuclear membrane areas were photographed at the same magnification (15000 x).

Morphometry and statistical analysis

Pore counting was done from prints of freeze-fracture negative micrographs. Fractured surface nuclear membranes and pores of nuclei were copied on a trans-

parent drawing paper and examined in a bit pad digitizing tablet and processed according to Peachey (1982), with a morphometric program to measure the areas of the fractured nuclear membranes and to count the number of nuclear pores in order to obtain the nuclear pore density. One-way ANOVA was used to compare the three nuclear samples among them. The level of significance was fixed as $P \leq 0.05$. Apoptosis figures were counted in TUNEL assay tissue slices, using a reticulate ocular under light microscopy. Ten microscopic areas from each corpus luteum were counted with a 70 x objective magnification. One-way ANOVA was also used in this case.

Results

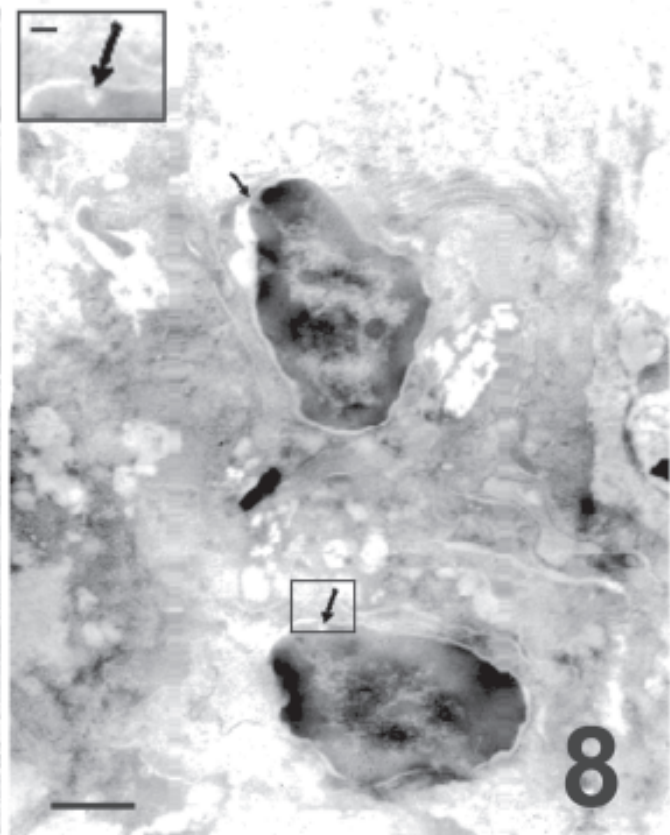
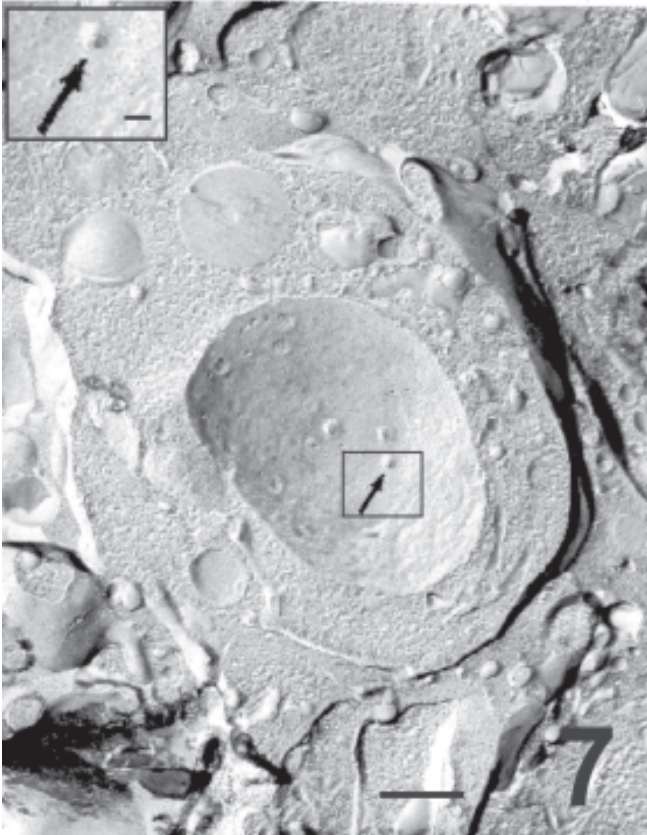
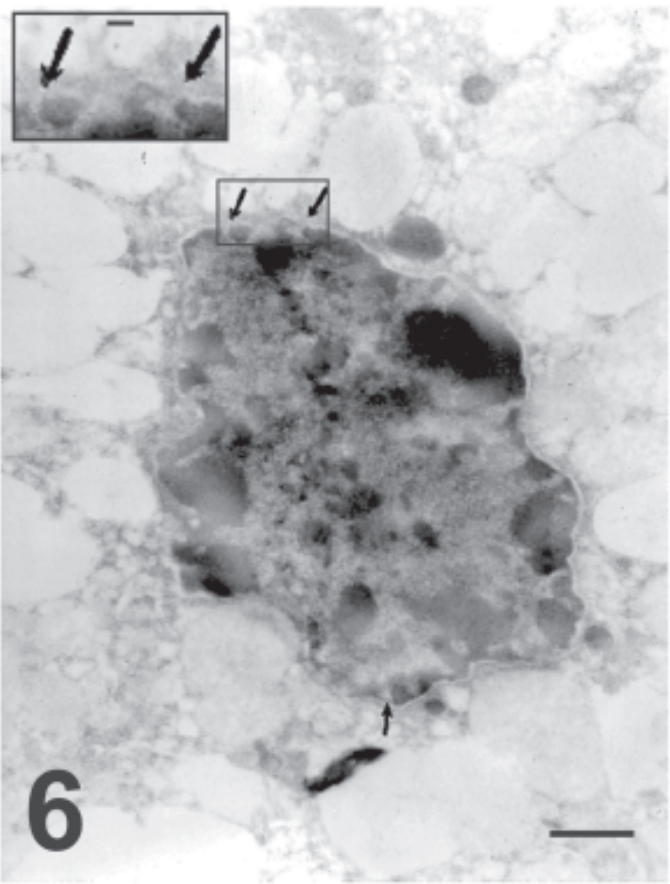
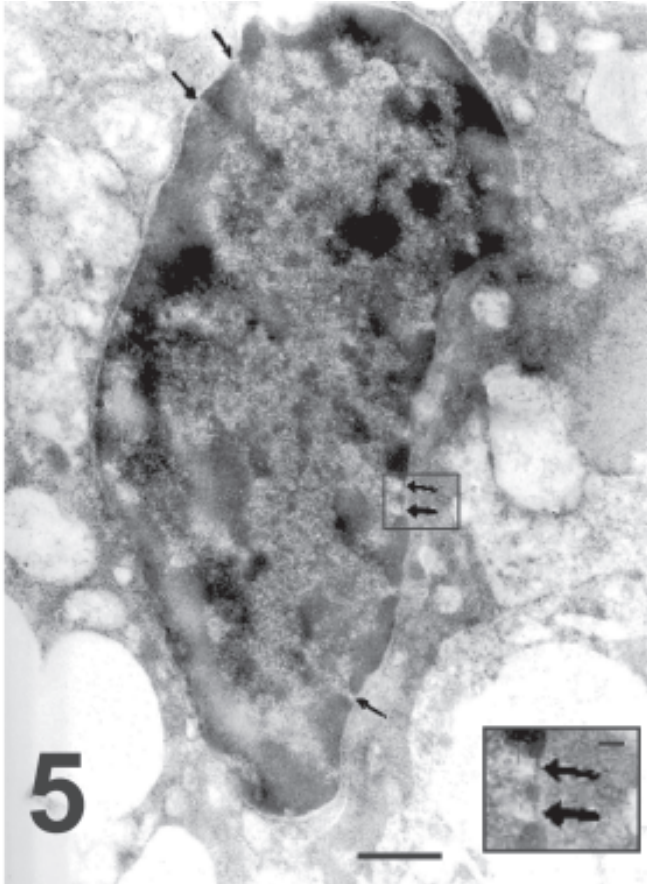
Normal endocrine luteal cells on day 15 of pregnancy show round (about 24 μm large), smoothly outlined nuclei with an even chromatin distribution (Fig. 1). By freeze-fracture their nuclear pores appear clearly defined and evenly distributed (Fig. 2). On the same day of pregnancy, however, a small number of degenerated, probably apoptotic nuclei were found. They exhibited small patches of condensed chromatin mostly margined on the nuclear envelope (Fig. 3), while nuclear pores were found in areas of rarefied chromatin. In freeze-fracture replicas, the nuclear pores were definitely reduced in number in the latter nuclei, although they appeared evenly distributed (Fig. 4) and they still presented a definite outline (Fig. 4, inset). By day 21 of pregnancy, the proportion of these nuclei, with similar pore features, definitely increased in both thin sections and freeze-fracture replicas.

FIGURE 5. Electron micrograph showing a more advanced chromatin condensation in a luteal cell on the fifth day after parturition. Nuclear pores are still observed (arrows) in the few remaining areas of dispersed chromatin. Bar represents 2 μm . The inset shows at higher magnification details of the nuclear pores (arrows), which coincide with thin spaces with dispersed chromatin. Bar represents 0.75 μm .

FIGURE 6. Thin section of a more advanced apoptosis to show the intense degenerate chromatin in small patches that now protrude on the nuclear envelope (this should be the first step in the formation of apoptotic bodies). Arrows indicate areas of nuclear pores. Bar represents 2 μm . The inset shows at higher magnification a nuclear area with poorly defined pores. Bar represents 0.75 μm .

FIGURE 7. Freeze fracture of apparently an apoptotic body. A small nuclear fragment surrounded by the body envelope displays nuclear pores (arrow). Day 5 after parturition and pup removal. Notice that their diameter is about 9 μm , clearly smaller than apoptotic nuclei in advanced stage. Bar represents 2 μm . Inset: An arrow indicates at higher magnification a nuclear pore. Bar represents 0.75 μm .

FIGURE 8. Thin section of a similar area of the previous figure. Two apparently apoptotic bodies display condensed, marginal chromatin patches, while small zones with dispersed chromatin are still associated with nuclear pores (arrows). Notice the apoptotic body size about 6-9 μm . Bar represents 2 μm . The inset shows at higher magnification a nuclear pore (arrow). Bar represents 0.75 μm .



Five days after parturition and pup removal, the degree of apoptosis and the reduction of pore density were even greater. Electron microscopy of thin sections showed an increment in chromatin condensation in many nuclei (Fig. 5) and it was frequently observed that the small chromatin patches shown in previous figures protrude on the nuclear envelope (Fig. 6). Also, numerous apparently apoptotic bodies are seen both in thin sections (Fig. 8) and in freeze fracture replicas (Figs. 7, 9 and 10). The outlines of the nuclear pores (Figs. 7, 8, 9 and 10, insets) appear blurred in these preparations.

The TUNEL assay confirmed that those degenerated nuclei were indeed apoptotic ones (Fig. 11). By the end of pregnancy (day 21) there was a definite increment of apoptosis frequency as compared to day 15

(Fig. 12) and which was correlated with a significant reduction of pore density (Fig. 13). Pup removal after parturition was followed by an even greater apoptosis frequency and by a drastic reduction of pore density (Figs. 12 and 13).

Discussion

In eukaryotic cells, the nucleus is surrounded by a double membrane system, the nuclear envelope, which is a highly specialized membrane that delineates the eukaryotic cell nucleus. It is composed of the inner and outer nuclear membranes, nuclear pore complexes and, in Metazoa, the nuclear lamina (Cohen *et al.*, 2001).

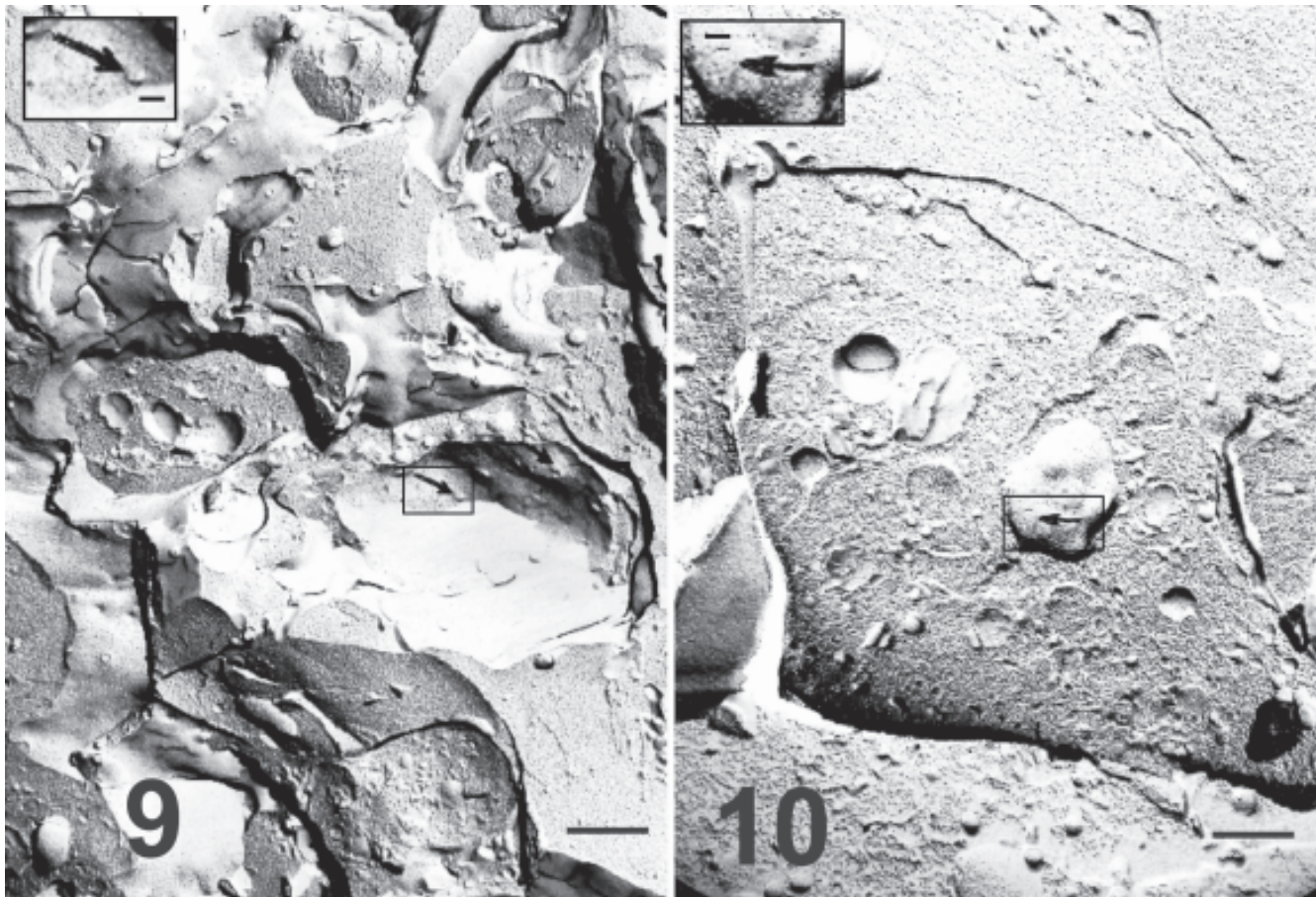


FIGURE 9. Freeze-fracture replica of an apoptotic body on day 5 after parturition and pup removal. A more advanced apoptotic body with very few nuclear pores (arrow) is shown. In this apoptotic stage nuclear pores appeared blurred. Notice the apoptotic body size, similar to the previous figure. Bar represents 2 μm . Inset: A nuclear pore at higher magnification is poorly defined (arrow). Bar represents 0.75 μm .

FIGURE 10. A still more advanced apoptotic body in a replica of a luteal cell on day 5 after parturition and pup removal. Apoptotic bodies are smaller in this terminal apoptotic stage with few almost undistinguishable nuclear pores (arrow). Bar represents 2 μm . Inset: the outline of the pore appears blurred at higher magnification (arrow), bar represents 0.75 μm .

The nuclear envelope not only regulates the trafficking of macromolecules between nucleoplasm and cytosol but also provides anchoring sites for chromatin and the cytoskeleton. Nuclear pores fuse the inner and outer nuclear membranes to form aqueous translocation channels that allow the free diffusion of small molecules and ions, as well as receptor-mediated transport of large macromolecules. Being the sole gateways for import and export to and from the nucleus, they regulate the nucleocytoplasmic transport of macromolecules in a highly selective manner to maintain cellular functions. The large size and complexity of these multimolecular assemblies, which are composed of approximately 30 different proteins (termed nucleoporins), present a major challenge for structural biologists (Hetzer *et al.*, 2005; Elad *et al.*, 2009).

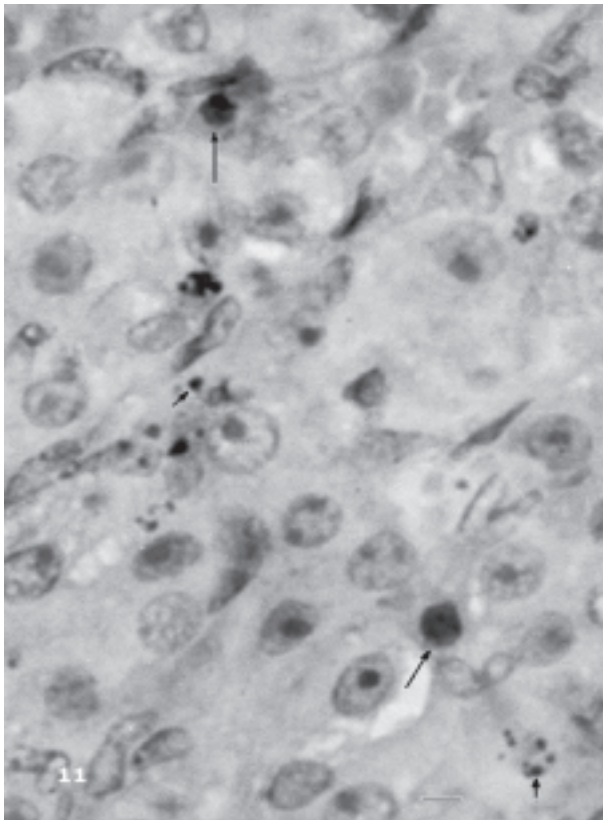


FIGURE 11. TUNEL labelling of a corpus luteum on day 5 after parturition and pup removal. Apoptosis is clearly observed in some nuclei (long arrows). Apoptotic fragmentation and the formation of numerous apoptotic bodies are also shown (short arrows). Non apoptotic nuclei are about 12-15 μm , apoptotic nuclei are about 7-12 μm and apoptotic bodies are about 2-5 μm large. Bar represents 20 μm .

Nuclear pores occurring in corpora lutea of pregnancy (days 15 and 21) show a definite decrease in number, but do not show aggregations sharply separated from pore-free areas, which is in contrast to other models of apoptosis (e.g., Falcieri *et al.*, 1994). Electron microscopy of thin-sections indicates, coincidentally with the examination of freeze-fracture replicas, only small irregular clumps of marginal heterochromatin condensations. However, small chromatin protrusions on the nuclear envelope (see Fig. 6) are frequently observed and indicate the first step in the formation of apoptotic bodies (Weedon *et al.*, 1979). After nuclear fragmentation and micronuclear formation, pores behave in the usual manner; we constantly observed their localization on the free chromatin areas (see Fig.8).

The occurrence of a certain degree of apoptosis on day 15 of pregnancy surprised us, since corpora lutea are fully functional on this day and progesterone levels decrease sharply only after day 19. Our findings of apoptotic cells on day 21 may be correlated with the sharp decrease of plasma progesterone levels observed after day 19 of pregnancy (Morishige *et al.*, 1973; Pepe and Rothchild, 1974). However, it is possible that luteal apoptosis is not only involved in luteal regression, but also in balancing proliferation in the regulation of development and growth of this ephemeral gland.

In the present study we present evidences that the apoptotic model of the corpus luteum, although different from the usual models in relation to the quantity of apoptotic chromatin associated to the nuclear envelope, follows the same characteristic behavior, *i.e.*, migrations of the nuclear pores toward the free chromatin areas, thus permitting nuclear/cytoplasm exchange even after certain degree of apoptosis. Our freeze-fracture observations corroborate these evidences providing the necessary morphometric analysis. An interesting aspect of the nuclear pores in freeze fractures observed by us in advanced stages of apoptosis (after parturition and pup removal) is that they are almost undistinguishable (Figs. 7, 8, 9, 10, insets). This aspect was seldom reported in the bibliography, and they were also interpreted as a failure of their function (Falcieri *et al.*, 1994).

Acknowledgements

This project was supported by the National Research Council of Argentina (CONICET, Argentina) and the Universidad Nacional de Cuyo, Mendoza, Argentina. The technical assistance of Eng. Jorge Ernesto Ibañez is highly appreciated.

Figure 12
Apoptotic Density

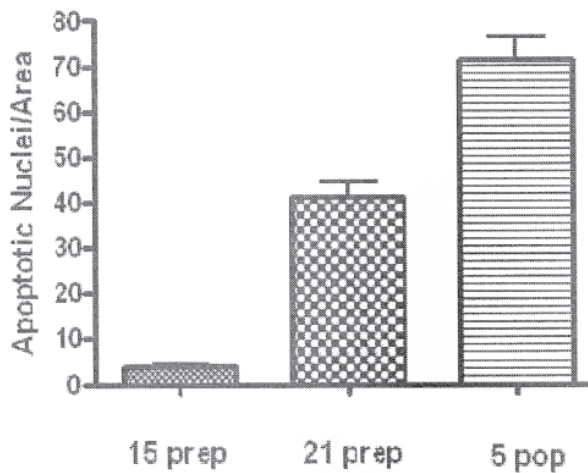


Figure 13
Nuclear Pore Density

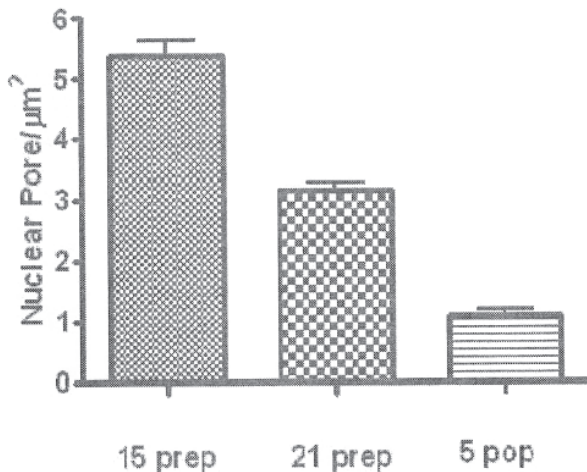


FIGURE 12. Percent of luteal nuclei showing TUNEL labeling on days 15 (15 prep) and 21 of pregnancy (21 prep), and on day 5 after parturition and pup removal (5 pop). Values are mean \pm SE. Differences were statistically significant among all groups.

FIGURE 13. Nuclear pore density (nuclear pores/ μm^2) in freeze fracture replicas on days 15 (15 prep) and 21 of pregnancy (21 prep), and on day 5 after parturition and pup removal (5 pop). Values are mean \pm SE. Differences were statistically significant among all groups.

References

- Aldrich HC, Pendland JC (1981). Nuclear pores during the cell cycle in a slime mold, *Physarum polycephalum*. *Tissue and Cell* **13**: 431-439.
- Cavicchia JC, Morales A (1992). Characterization of germ cell nuclei in freeze-fracture replicas of seminiferous tubules isolated by transillumination at various stages of the spermatogenic cycle. *Tissue and Cell* **24**: 75-84.
- Cavicchia JC, Sacerdote FL, Morales A, Zhu BC (1998). Sertoli cell nuclear pore number changes in two stage sets of the rat spermatogenic cycle. *Tissue and Cell* **30**: 268-273.
- Cohen M, Gruenbaum Y, Lee K, Wilson K (2001). Transcriptional repression, apoptosis, human disease and the functional evolution of the nuclear lamina. *Trends in Biochemical Sciences* **26**: 41-47.
- Elad N, Maimon T, Frenkiel-Krispin D, Lim RY, Medalia O (2009). Structural analysis of the nuclear pore complex by integrated approaches. *Current Opinions in Structural Biology* **19**: 226-232.
- Falcieri E, Gobbi P, Cataldi A, Zamai L, Faenza I, Vitale M (1994). Nuclear pores in the apoptotic cell. *The Histochemical Journal* **26**: 754-763.
- Friend DS, Fawcett DW (1974). Membrane differentiations in freeze-fractured mammalian sperm. *Journal of Cell Biology* **63**:641-664.
- Gavrieli Y, Sherman Y, Ben Sasson SA (1992). Identification of programmed cell death in situ via specific labeling of nuclear DNA fragmentation. *Journal of Cell Biology* **119**: 493-501.
- Hetzer MW, Walther TC, Mattaj IW (2005). Pushing the envelope: structure, function, and dynamics of the nuclear periphery. *Annual Review of Cellular and Developmental Biology* **21**: 347-80.
- Karnovsky MJ (1971). Use of ferrocyanide-reduced osmium in electron microscopy. *Journal of Cell Biology* **51**: 146A.
- Maul GG, Maul HM, Scogna JE, Lieberman GS, Stein B, Hsu YL, Borum TW (1972). Time sequence of nuclear pore formation in phytohemagglutinin-stimulated lymphocytes and in HeLa cells during the cell cycle. *Journal of Cell Biology* **55**: 433-447.
- Morales A, Mohamed F, Cavicchia JC (2007). Apoptosis and blood-testis barrier during the first spermatogenic wave in the pubertal rat. *Anatomical Record* **290**: 206-214.
- Morishige WK, Pepe GJ, Rothchild I (1973). Serum luteinizing hormone, prolactin and progesterone levels during pregnancy in the rat. *Endocrinology* **92**: 1527-530.
- Peachey LD (1982). A simple digital morphometry system for electron microscopy. *Ultramicroscopy* **8**: 253-262.
- Pepe GJ, Rothchild I (1974). A comparative study of serum progesterone levels in pregnancy and in various types of pseudopregnancy in the rat. *Endocrinology* **95**: 1275-279.
- Reynolds ES (1963). The use of lead citrate at high pH as electroopaque stain in electron microscopy. *Journal of Cell Biology* **17**: 208-212.
- Sinha Hikim AP, Lue Y, Swerdloff RS (1997). Separation of germ cell apoptosis from toxin-induced cell death by necrosis using in situ end-labeling: histochemistry after glutaraldehyde fixation. *Tissue and Cell* **29**: 487-493.
- Spurr AR (1969). A low viscosity epoxy resin embedding medium for electron microscopy. *Journal of Ultrastructural Research* **26**: 31-43.

- Takiguchi K, Sugino N, Esato K, Karube-Harada A, Sakata A, Nakamura Y, Ishikawa H, Kato H (2004). Differential Regulation of Apoptosis in the corpus luteum of pregnancy and newly formed corpus luteum after parturition in rat. *Biology of Reproduction* **70**: 313-318.
- Telleria CM, Goyeneche AA, Cavicchia JC, Stati AO, Deis RP (2001). Apoptosis induced by antigestagen RU486 in rat corpus luteum of pregnancy. *Endocrine* **15**: 147-155.
- Weedon D, Searle J, Kerr JFR (1979). Apoptosis. Its nature and implications for dermatopathology. *American Journal of Dermatopathology* **1**: 133-144.

